Cell Transplantation
2018, Vol. 27(3) 485–500

DOI: 10.1177/0963689718755404
journals.sagepub.com/home/cll
SAGE

Serum-mediated Activation of Bone Marrow–derived Mesenchymal Stem Cells in Ischemic Stroke Patients: A Novel Preconditioning Method

Gyeong Joon Moon[1,2,3], Yeon Hee Cho[1,4], Dong Hee Kim[1,5], Ji Hee Sung[1,4], Jeong Pyo Son[1,5], Sooyoon Kim[1,4], Jae Min Cha[6], and Oh Young Bang[1,5,7]

Abstract

Stroke induces complex and dynamic, local and systemic changes including inflammatory reactions, immune responses, and repair and recovery processes. Mesenchymal stem cells (MSCs) have been shown to enhance neurological recovery after stroke. We hypothesized that serum factors play a critical role in the activation of bone marrow (BM) MSCs after stroke such as by increasing proliferation, paracrine effects, and rejuvenation. Human MSCs (hMSCs) were grown in fetal bovine serum (FBS), normal healthy control serum (NS), or stroke patient serum (SS). MSCs cultured in growth medium with 10% SS or NS exhibited higher proliferation indices than those cultured with FBS ($P < 0.01$). FBS-, NS-, and SS-hMSCs showed differences in the expression of trophic factors; vascular endothelial growth factor, glial cell–derived neurotrophic factor, and fibroblast growth factor were densely expressed in samples cultured with SS ($P < 0.01$). In addition, SS-MSCs revealed different cell cycle– or aging-associated messenger RNA expression in a later passage, and β-galactosidase staining showed the senescence of MSCs observed during culture expansion was lower in MSCs cultured with SS than those cultured with NS or FBS ($P < 0.01$). Several proteins related to the activity of receptors, growth factors, and cytokines were more prevalent in the serum of stroke patients than in that of normal subjects. Neurogenesis and angiogenesis were markedly increased in rats that had received SS-MSCs ($P < 0.05$), and these rats showed significant behavioral improvements ($P < 0.01$). Our results indicate that stroke induces a process of recovery via the activation of MSCs. Culture methods for MSCs using SS obtained during the acute phase of a stroke could constitute a novel MSC activation method that is feasible and efficient for the neurorestoration of stroke.

Keywords

stroke, mesenchymal stem cells, stem cell activation

Introduction

Alongside cancer and coronary heart disease, stroke is a leading cause of death; in addition, it is the most common cause of physical disability in adults. Stroke induces complex and dynamic systemic and local changes because substances in the infarcted brain flow into the peripheral blood system across the damaged blood–brain barrier and may trigger systemic responses[1]. Systemic changes include inflammatory reactions, immune responses, and repair and recovery processes.

Mesenchymal stem cells (MSCs) are multipotent adult stem cells that are present in various tissues, including bone marrow (BM), adipose, and the umbilical cord, and have the

[1] Translational and Stem Cell Research Laboratory on Stroke, Sungkyunkwan University, Jongno-gu, Seoul, South Korea
[2] Stem Cell and Regenerative Medicine Institute, Samsung Medical Center, Gangnam-gu, Seoul, South Korea
[3] School of Life Sciences, BK21 Plus KNU Creative BioResearch Group, Kyungpook National University, Buk-gu, Daegu, South Korea
[4] Samsung Biomedical Research Institute, Samsung Medical Center, Gangnam-gu, Seoul, South Korea
[5] Samsung Advanced Institute for Health Sciences and Technology, Sungkyunkwan University, Jongno-gu, Seoul, South Korea
[6] Medical Device Research Center, Research Institute for Future Medicine, Samsung Medical Center, Seoul, Republic of Korea
[7] Department of Neurology, Samsung Medical Center, Sungkyunkwan University, Jongno-gu, Seoul, South Korea

Submitted: November 28, 2016. Revised: January 01, 2018. Accepted: January 02, 2018.

Corresponding Author:
Oh Young Bang, Department of Neurology, Samsung Medical Center, Sungkyunkwan University, 50 Irwon-dong, Gangnam-gu, Seoul 135-710, South Korea.
Email: ohyoung.bang@samsung.com

capacity for self-renewal and differentiation; studies have shown that MSCs can enhance neurological recovery after stroke. In particular, BM is known to be regulated by the brain through pathways that include the sympathetic nervous system and systemic inflammation and is activated after a stroke[2,3]. Thus, there may be biological or physiological changes in stroke patients' BM-MSCs. Preclinical studies that compared either BM-MSCs or mononuclear cells (MNCs) between normal and ischemic stroke animals showed that MSCs/MNCs derived from stroke-model rats exhibited increased trophic factor gene expression and enhanced restorative properties with regard to endogenous brain parenchymal cells[4,5]. These preclinical results suggest that serum obtained from the acute phase of a stroke could activate allogeneic MSCs ex vivo.

We hypothesized that the activated BM-MSCs by serum after stroke promote brain recovery. Therefore, we investigated the biological characteristics of MSCs, including their proliferation capacity and senescence state, and trophic supports grown with serum obtained from patients with ischemic stroke. In addition, we evaluated the circulating factors of stroke patients that may be related to the activation of MSCs.

Materials and Methods

In this study, all human subject research was approved by our local institutional review board (*Samsung Medical Center Institutional Review Board, Approval No. SMC 2011-10-047-047*). All patients or guardians of patients provided written informed consent to participate in this study. All animal experiments were approved by Institutional Animal Care and Use Committee (IACUC) of Samsung Biomedical Research Institute (Approval No. 201300117002) and performed under the Institute of Laboratory Animal Resources guidelines. All animals were maintained in compliance with the relevant laws and institutional guidelines of Laboratory Animal Research Center (AAALAC International approved facility, No. 001003) at the Samsung Medical Center. The experimental time line was provided in Online Supplementary Fig. 1.

Preparation of Serum

Human serum was collected from ischemic stroke patients enrolled in the trial[6] within 90 d after onset ($n = 9$, 30.4 ± 18.1 d) and from healthy normal subjects ($n = 8$). Aliquots of serum were stored at -70 °C until ready for use. Patient basal characteristics are provided in Table 1.

MSC Culture

Human MSCs (hMSCs) at passage 2 were purchased from Lonza, Basel, Switzerland (Cat No. PT-2501). hMSCs were grown in Dulbecco's modified Eagle's medium (DMEM, Invitrogen, Carlsbad, CA, USA) with 10% fetal bovine serum (FBS; Hyclone, Victoria, Australia) for the first passage. Then changed to medium with 10% FBS, 10% normal healthy control serum (NS), or 10% stroke patient serum (SS). hMSCs were used at passage 5 to 10 for in vitro study. hMSCs of passage 5 were transplanted to study their therapeutic effects.

In this study, the phenotype of the cells is confirmed by flow cytometry analysis (FCM, fluorescent-activated cell sorting Calibur; BD Biosciences, Franklin Lakes, NJ, USA). The following CD surface markers were tested: CD90, CD73 (positive surface marker, BD Biosciences), CD45, and CD34 (negative surface marker, BD Biosciences). FCM data were acquired on a Calibur flow cytometer using Cell Quest software version 6.0 (BD Biosciences).

Calculation of Population Doubling

Cumulative population doubling level (CPDL) in continual subculture and growth from a known number of cells was calculated to determine the proliferative potential of hMSCs. The CPDL at each subcultivation was calculated from the cell count using the formula $N_i + \ln(N_f/N_i)/\ln 2$, where N_i and N_f are the initial and final cell numbers, respectively[7]. The population doubling time (PDT) was calculated using the equation $T(\mathrm{h}) \times \ln 2/\ln(N_f/N_i)$, where $T(\mathrm{h})$ is the cell culture time[8].

Real-time Quantitative Polymerase Chain Reaction (RT-qPCR)

Total RNA was extracted using Trizol™ (Gibco, Waltham, MA, USA). cDNA was synthesized from 2 μg of total RNA using oligo $d(T)_{16}$ primers (Promega, Madison, WI, USA) and the Omniscript RT kit (Qiagen, Hilden, Germany). For RT-qPCR analysis of vascular endothelial growth factor (VEGF), glial cell–derived neurotrophic factor (GDNF), fibroblast growth factor 2 (FGF2), and glyceraldehyde 3-phosphate dehydrogenase, SYBR Green assays were performed using SYBR Green PCR Master Mix (Applied Biosystems, Foster City, CA, USA) on an ABI Prism 7900 real-time polymerase chain reaction (RT-PCR) system (Applied Biosystems). Primers and probes were obtained commercially (Bioneer, Daejeon, South Korea) and are described in Online Supplementary Table 1.

RT-PCR Arrays

Pathway-specific PCR arrays (cell cycle array, aging array, SABiosciences, Qiagen) were used according to the manufacturer's instructions. Data were analyzed using the manufacturer's software. Biological pathway analysis was performed using the Functional Enrichment Analysis tool (FunRich version 3.0, http://www.funrich.org)[9].

β-galactosidase Staining

β-galactosidase staining was performed using a senescence-associated β-galactosidase (SA-β-gal) staining kit (Cell

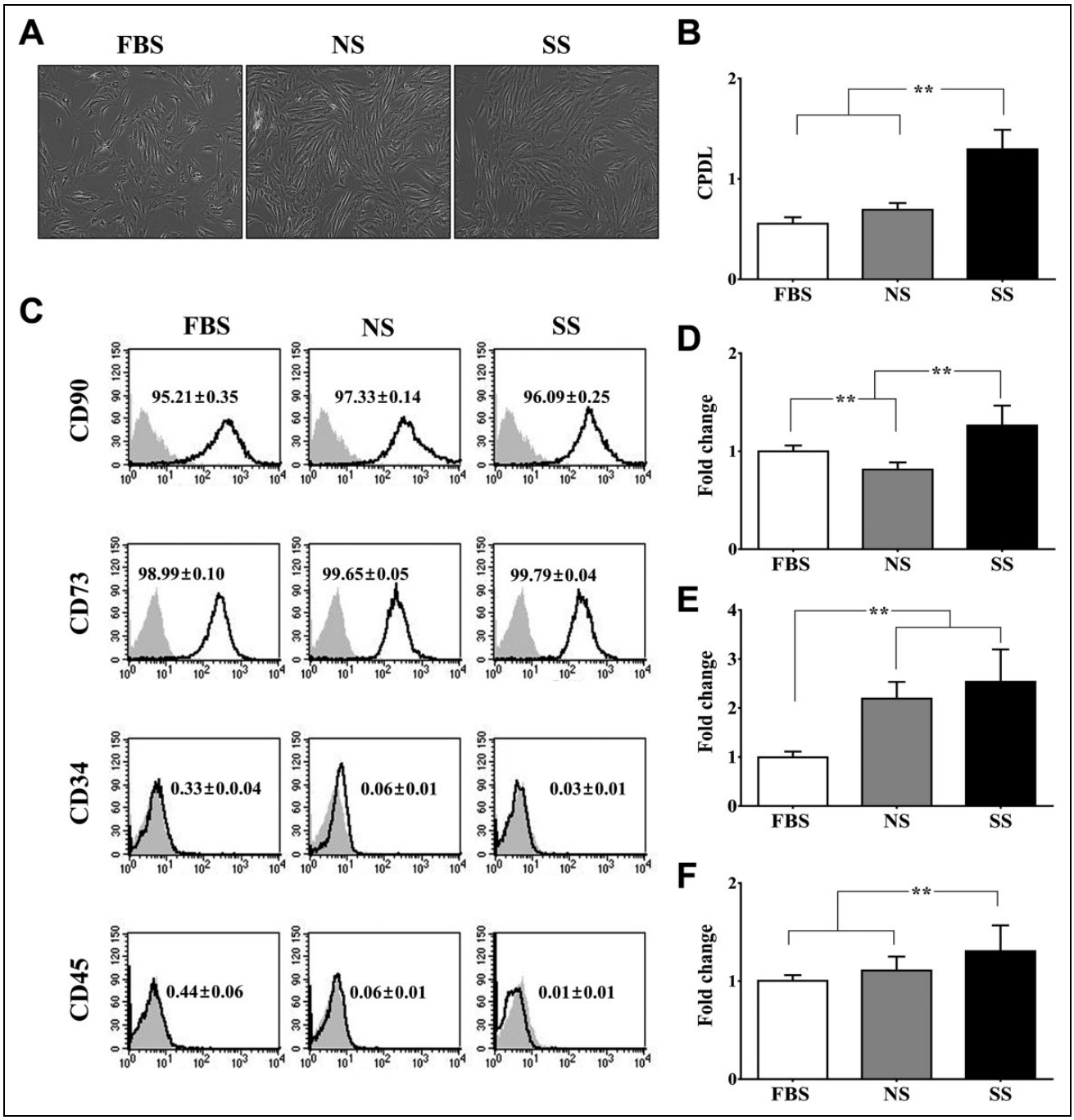

Fig. 1. Evaluation of phenotypic characteristics of mesenchymal stem cells (MSCs). (A) Representative phase contrast images of human MSCs (hMSCs) expanded with the different serums. (B) Cumulative population doubling level of hMSCs cultured in Dulbecco's modified Eagle's medium with 10% fetal bovine serum (FBS), control serum (NS), and stroke patient serum (SS). (C) Fluorescent-activated cell sorting analysis of hMSCs cultured with different types of serum. Quantitative analysis of the percentages of cells expressing CD90, CD73 (positive markers), and CD34, CD45 (negative markers). The relative expression levels of both human vascular endothelial growth factor (D) and human fibroblast growth factor (F) were significantly increased in SS-hMSCs than FBS-hMSCs or NS-hMSCs. Human glial cell–derived neurotrophic factor (E) expression level was significantly lower in FBS-hMSCs than NS-hMSCs and SS-hMSCs. All data are presented as mean + SD (**$P < 0.01$, $n = 6$).

Signaling Technology, Danvers, MA, USA), according to the manufacturer's instructions. Briefly, the cells were fixed with fixation solution for 15 min at room temperature, washed with phosphate buffer solution (PBS), and stained with β-galactosidase staining solution overnight at 37 °C in a dry incubator. Images were acquired with an EVOS

Table 1. Patient's Baseline Characteristics.

Characteristics	Stroke Patients	Healthy Subjects	*P* Value
Number of patients	9	8	
Age, year (SD)	71.11 (3.14)	67.25 (13.28)	0.409
Sampling time (mean + SD)	30.4 ± 18.1 d		
Gender, *N* (% of female)	4 (44.4%)	4 (50%)	0.819
NIHSS (SD)	16.71 (4.89)		
Infarct volume, mL (SD)	13.57 (8.73)		
Risk factors, *N*			
Hypertension	6	1	0.024
Diabetes mellitus	3	0	0.072
Hyperlipidemia	2	0	0.156
Atrial fibrillation	3	0	0.072
Current smoking	2	0	0.156
BMI, kg/m^2 (SD)	24.86 (1.97)	24.98 (3.22)	0.957

Abbreviations: SD, standard deviation; BMI, Body Mass Index; NIHSS, NIH Stroke Scale.

microscope (Advanced Microscopy Group [AMG], Mill Creek, WA, USA).

Protein Array Analysis

Antibody array experiments were performed using the RayBio Biotin Label-based Human Antibody Array (AAH-BLG-1-4, RayBiotech, Inc., Norcross, GA, USA). A total of 507 different human proteins were detected including cytokines, chemokines, growth factors, differentiation factors, angiogenic factors, adipokines, adhesion molecules, matrix metalloproteases, binding proteins, inhibitors, and soluble receptors. Antibody analyses were performed according to recommended protocols. The signals were scanned by a GenePix 4000B laser scanner (Agilent, Santa Clara, CA, USA). Normalization was done using the signal of internal controls on each array chip. Significance testing was done by *t* test and fold change was cut off at 1.5. Molecular function analysis was performed using FunRich[9].

Middle Cerebral Artery Occlusion Model

We induced transient middle cerebral artery occlusion (tMCAO) using a previously described intraluminal vascular occlusion method that was modified in our laboratory[10]. Briefly, anesthesia was induced in male Sprague-Dawley rats (7 to 8 wk, 250 to 300 g, Orient Bio Inc., Seongnam, South Korea) with 4% isoflurane and maintained with 1.5% isoflurane in 70% N_2O and 30% O_2. The temperature was maintained at 37.0 °C to 37.5 °C (measured rectally) with heating pads throughout the surgery and occlusion period. A 4-0 surgical monofilament nylon suture with a rounded tip was advanced from the left common carotid artery into the lumen of the internal carotid artery until it blocked the origin of the middle cerebral artery. Reperfusion was allowed 90 min after tMCAO by withdrawing the suture until the tip cleared the lumen of the common carotid artery. Rats with hemorrhagic transformation or subarachnoid hemorrhage caused by rupture of the intracranial artery and rats without observable neurological deficits following MCAO were excluded from further analyses.

The regional cerebral blood flow (rCBF) in the MCA territory was measured transcranially by laser Doppler flowmetry (Moor Instruments, Wilmington, DE, USA) via probes placed on ipsilateral hemisphere. CBF was recorded continuously during 10 min of baseline recording, 10 min of ischemia, and 15 min of reperfusion. The reduction in CBF was calculated as percentage of baseline. Rats that failed to show at least 70% rCBF reduction were also excluded from further analyses.

In a separate experiment, physiological parameters (blood pressure, pH, pCO_2, pO_2, Na, K, Ca, glucose, hematocrit, and hemoglobin) were measured at 4 different time points (before MCAO, at 10 min after MCAO, at 10 min after reperfusion, and after treatments, $n = 5$ per group). Femoral artery cannulation was performed for arterial pressure monitoring and arterial blood sampling with heparin tube. The arterial blood pressure was continuously monitored during operation, and arterial blood samples were obtained 5 min prior to ischemia (baseline), 10 min following reperfusion, and 10 min following treatment for blood gas analysis (i-STAT, Abbott Diagnostics, Lake Forest, IL, USA).

hMSC Transplantation

hMSCs were harvested after being cultured in DMEM with 10% FBS, 10% NS, or 10% SS by passage 3 to 5. hMSCs (2×10^6 cells) were administrated 1 d after tMCAO. The control group received PBS after tMCAO. The suspended hMSCs were slowly injected with a 1-mL syringe into the tail vein of the rats. In this study, a total of 40 rats were equally randomized into 4 groups: the PBS, FBS-hMSCs, NS-hMSCs, and SS-hMSCs. Four animals (2 animals in the PBS group, 1 animal in the NS-hMSCs and SS-hMSCs groups, respectively) died within 24 h after tMCAO, and these animals were excluded. Two animals without observable neurological deficits were excluded in the FBS-hMSCs group. One animal with subarachnoid hemorrhage was excluded each in the NS-hMSCs and SS-hMSCs groups. A total of 32 animals were included in the final analysis ($n = 8$ in each treatment group).

Functional Tests

In all animals, modified neurological severity scores (mNSS) were performed before tMCAO, and 1, 3, 7, 14, 21, 28, and 35 d afterward, by an investigator who was blinded to the experimental groups. The mNSS were calculated as a measure of motor, sensory, and reflex function and balance, using a modified version of the sensory tests[11]. The total mNSS were scaled from 0 to 18 (normal = 0, maximal deficit = 18). The mNSS were determined by measuring responses to being raised by the tail (subtotal score = 0 to

3: forelimb flexion = 0 to 1, hind-limb flexion = 0 to 1, and head movement over 101° to the vertical axis within 30 s = 0 to 1), results of sensory tests (subtotal score = 0 to 12: visual placement of forelimbs = 0 to 3, tactile placement of forelimbs = 0 to 3, proprioceptive adduction of hind limbs = 0 to 3, and tactile placement of hind limbs = 0 to 3), and beam balance tests (subtotal score = 0 to 6: balances with steady posture = 0, grasps side of beam = 1, hugs beam and 1 limb falls down = 2, hugs beam and 2 limbs fall down or spins over 60 s = 3, attempts to balance on beam but falls off over 40 s = 4, attempts to balance on beam but falls off over 20 s = 5, and falls off and no attempt to balance or hang onto beam within 20 s = 6).

Acquisition and Analysis of Magnetic Resonance (MR) Images

MR image analysis was performed using a 7T small animal MR scanner (70/20 USR; Bruker BioSpin, Billerica, MA, USA). A quadrature birdcage coil (inner diameter = 72 mm) was used for excitation, and an actively decoupled 4-channel-phased array surface coil was used for receiving the signal. MR images including T2-weighted image were acquired 1 d and 2 wk after onset of stroke under isoflurane anesthesia (5% for induction, 2% for maintenance). T2-weighted image was acquired using a turbo rapid acquisition with refocusing echoes (Turbo RARE) sequence with the following parameters: repetition time/echo time = 3,000/60 ms, field of view = 30×30 mm^2, image matrix = 192×192, and in-plane resolution = $0.156 \times 0.156 \times 0.75$ mm^3.

T2-weighted images were performed to estimate the ischemic lesion and lateral ventricular volume. The lesion area on each slice of T2-weighted image was specified by those pixels with a T2 value higher than the mean plus twice the standard deviation (mean + SD) measurements provided by the normal tissue on the contralateral side[12]. Whole infarct volume was obtained by multiplying the total lesion slices times the slice thickness. Lateral ventricular volumes were delineated from 8 contiguous T2-weighted images with reference to Paxinos stereotaxic rat brain atlas[13] to measure whether stem cell therapy prevents atrophy within peri-infarct area and secondary dilations of the adjacent ventricle[14]. Whole lateral ventricular volume was obtained by multiplying the total lesion slices times the slice thickness. The volume of the ischemic infarct and lateral ventricle was normalized to the volume of 1 d for compensation of individual bias.

Immunostaining

Five weeks after treatment, animals were sacrificed and subjected to transcardial perfusion with PBS and 4% paraformaldehyde. Brains were removed, stored in 4% paraformaldehyde at 4 °C overnight, and immersed in 30% sucrose for 3 to 4 d at 4 °C. Brains were then frozen rapidly in powdered dry ice and stored at −70 °C. Frozen brains were sectioned coronally between 3 and 4 mm posterior to the bregma to a thickness of 18 μm using a Cryocut Microtome (Leica Microsystems). The neurogenetic and angiogenetic effects of hMSCs were measured by immunofluorescence staining as previously described[10]. All rats received 5-bromo-2′-deoxyuridine (50 mg/kg, intraperitoneal, BrdU; Roche Holding AG, Basel, Switzerland) injections per day for the last week. Neurogenesis and angiogenesis effects were calculated using immunostaining with mouse anti-BrdU (diluted 1:50, Abcam, Cambridge, United Kingdom)/rabbit anti-doublecortin (anti-DCX, diluted 1:200, Abcam) or rabbit anti–von Willebrand factor (anti-vWF, diluted 1:200, Chemicon, Temecula, CA, USA). Images were acquired with an EVOS fl microscope (Advanced Microscopy Group). The number of BrdU/DCX double-positive cells was measured with Image (National Institutes of Health, Bethesda, MD, USA). The area of vWF was analyzed using Multi Gauge (Fuji Photo Film Co. Ltd., Tokyo, Japan).

Statistical Analysis

All measurements were performed by an investigator who was blinded to the experimental groups. In all assays, a total of 3 to 6 independent and separate experiments were performed to assess the different serum source supplements, and results were expressed as mean + SD. Statistical differences between groups were evaluated using the independent *t* test, 2-way analysis of variance (ANOVA) for repeated measures, and Tukey's post hoc analysis. *P* values <0.05 were considered statistically significant. Statistical analyses were performed using a commercially available software package, SPSS (SPSS Inc., Chicago, IL, USA). Graphs were drawn using Graph Pad Prism (Graph Pad Software, La Jolla, CA, USA).

Results

Baseline Characteristics of Study Human Subjects

The baseline clinical characteristics and laboratory findings are summarized in Table 1. There was no significant difference in age, gender, and risk factors between the groups, with exception of hypertension, which was more prevalent in the stroke patient group ($P = 0.024$).

Characteristics of hMSCs

The phenotypic characteristics of hMSCs were compared after they had been cultured in DMEM with 10% FBS (FBS-hMSCs), 10% NS (NS-hMSCs), or 10% SS (SS-hMSCs). The morphology and CD surface markers did not differ between the groups (CD90-, CD73-positive: ≥95%; CD34-, CD45-positive: ≤1%; Fig. 1A and C). The CPDLs of SS-hMSCs and NS-hMSCs were significantly higher than those of FBS-hMSCs (Fig. 1B; $^{**}P < 0.01$). The SS-hMSCs showed a significantly higher expression of VEGF and FGF2 than FBS-hMSCs or NS-hMSCs (Fig. 1D and E; $^{**}P < 0.01$). In

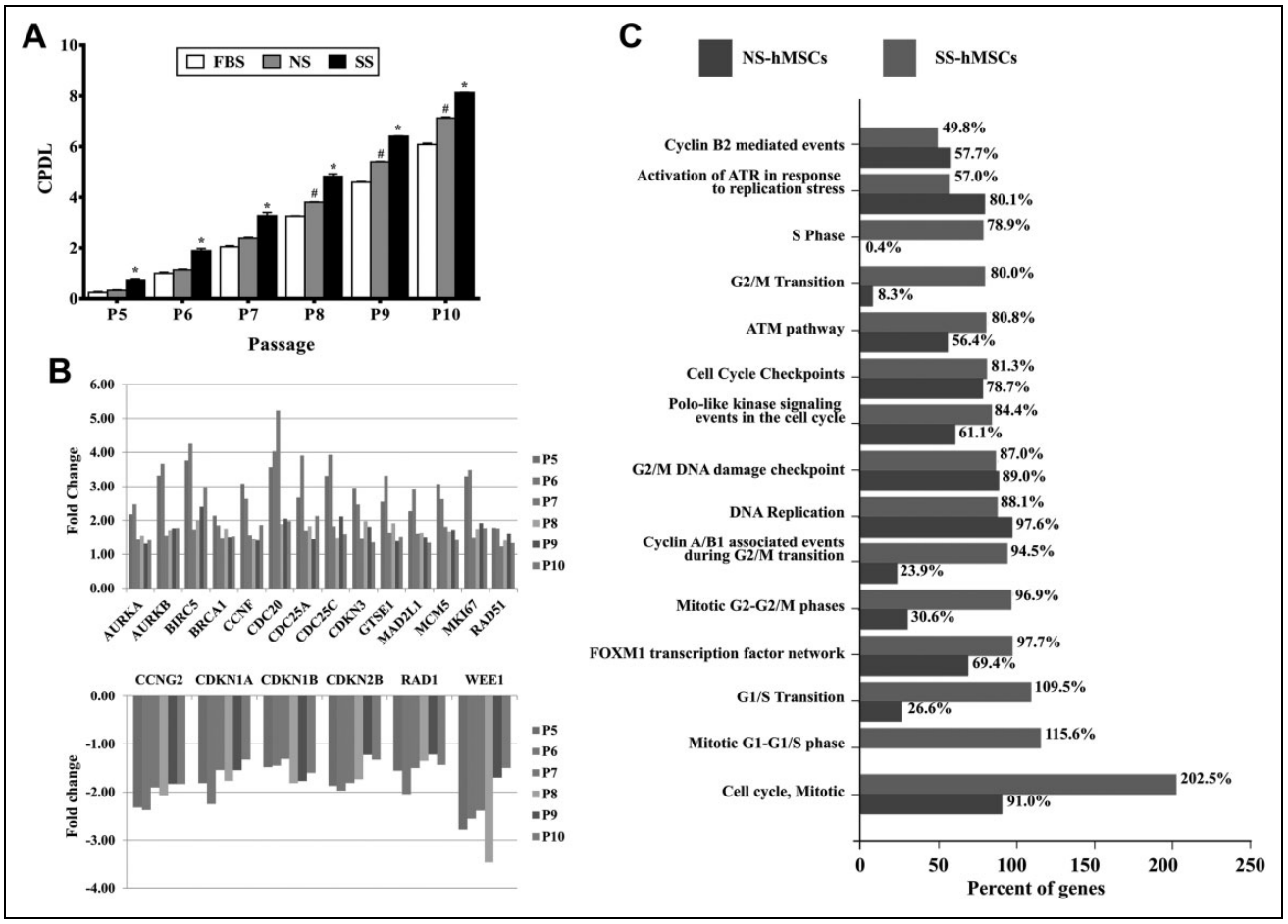

Fig. 2. Comparison of proliferation capacity. (A) Cumulative population doubling level of fetal bovine serum human mesenchymal stem cells (hMSCs), normal healthy control serum (NS) hMSCs, and stroke patient serum (SS) hMSCs by passage 5 to 10. (B) Bar charts illustrating the fold change of cell cycle–associated messenger RNA expression in SS-hMSCs relative to NS-hMSCs at P5 to P10, with cutoff values of $P < 0.05$ and 1.5-fold change. (C) Comparison of biological pathway enriched between NS-hMSCs and SS-hMSCs using the FunRich software.

addition, GDNF expression was significantly greater in SS-hMSCs than in FBS-hMSCs (Fig. 1F; $^{**}P < 0.01$).

Regulation of Cell Cycle–associated Messenger RNA (mRNA) Expression

The CPDL of SS-hMSCs was significantly higher than those of FBS- or NS-hMSCs at passages 5 to 10, and the CPDL of NS-hMSCs was significantly higher than that of FBS-hMSCs at passages 8 to 10 (Fig. 2A; $^{*}P < 0.01$, $\#P < 0.01$, respectively). The cell cycle–related mRNA expression profiles were analyzed to explore the underlying cellular mechanisms further. The expression patterns of cell cycle–associated mRNA became further differentiated between SS- and NS-hMSCs relative to FBS-hMSCs as the passage number increased. The expression of cell proliferation markers such as *MKI67*, *AURKA*, and *AURKB* were upregulated in SS-hMSCs. In addition, the expressions of *BRCA1* (tumor suppressor), *BIRC5* (survivin, apoptosis inhibitor), *MCM5*, *RAD51* (DNA repair), *CCNF*, *CDC20*, *CDC25A*, *CDC25C*, *CDKN3*, and *GTES1* (cell cycle checkpoint) in SS-hMSCs were greater, whereas the expressions of *CCNG2*, *CDKN1A*, *CDKN1B*, *CDKN2B*, *RAD1*, and *WEE1* (cell cycle inhibitor) were downregulated (Fig. 2B). Interestingly, functional enrichment analysis showed that the proliferative phase–associated mRNA abundance in SS-hMSCs was involved in the S phase (78.5%), G2/M transition (80.0%), G1/S transition (109.5%), the mitotic G1-G1/S phase (115.6%), cell cycle, and mitotic (202.5%; Fig. 2C).

Reversal of Cellular Senescence

A SA-β-gal assay was performed at the late stages (passage 8 to 10) to compare senescence status. The number of SA-β-gal-positive cells with blue staining continuously increased in both FBS-hMSCs and NS-hMSCs as the passage number increased. However, the number of SA-β-gal-positive cells significantly decreased in SS-hMSCs at passage 8 compared to FBS-hMSCs. This attitude maintained through passage 8 to 10 ($^{**}P < 0.01$, $^{*}P < 0.05$, Fig. 3A and B).

The aging-associated mRNA expression differences were observed in SS-hMSCs or NS-hMSCs relative to FBS-

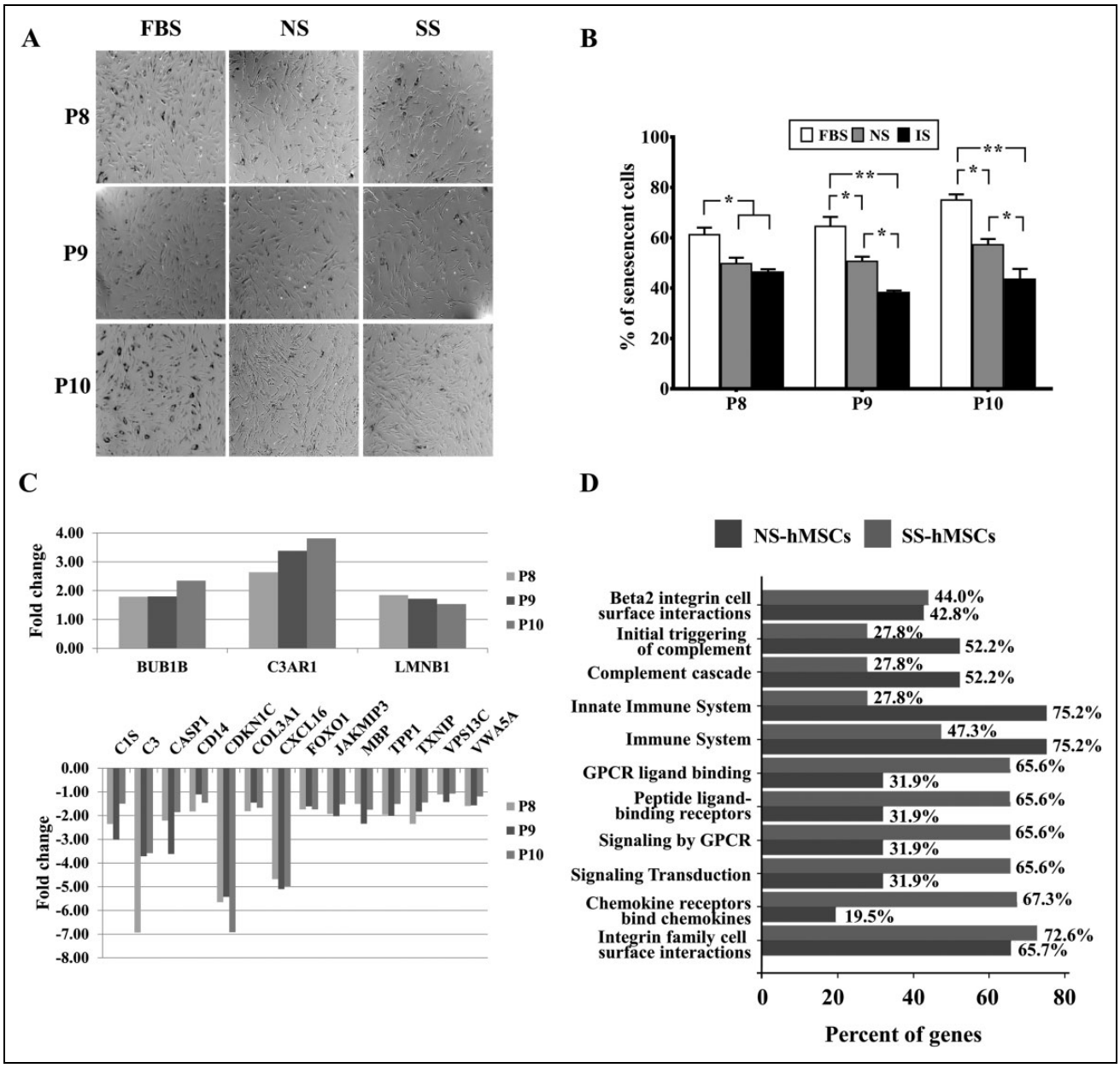

Fig. 3. Comparison of cellular senescence. (A) Representative images of senescence-associated β-gal staining in fetal bovine serum (FBS) human mesenchymal stem cell (hMSCs), NS-hMSCs, and SS-hMSCs at passages 8 to 10. (B) Quantitative analysis of senescence expressed as the percentage of positively stained cells. The absolute number of blue-stained cells was counted in 6 fields per well. The data are presented as mean + SD (**$P < 0.01$, $n = 6$). (C) messenger RNA expression in stroke patient serum (SS) hMSCs relative to normal healthy control serum (NS) hMSCs at P8 to P10, with cutoff values of $P < 0.05$ and 1.5-fold change. (D) Comparison of biological pathway enriched between NS-hMSCs and SS-hMSCs using the FunRich software.

hMSCs. The expressions of *BUB1b*, *LMNB1* (senescence inhibitor), and *C3AR1* (inflammation response) were greater in SS-hMSCs, whereas the expressions of *C1S*, *C3*, *CD14* (inflammation response), *CASP1* (apoptosis), *CDKN1C* (cell cycle checkpoint), *COL3A*, *CXCL16*, *FOXO1*, *JAKMIP3*, *MBP*, *TPP1*, *TXN1P*, *VPS13C*, and *VWA5A* were downregulated in SS-hMSCs (Fig. 3C). The expressions of *TMEM33* and *TMEM135* were lower in NS-hMSCs compared to SS-MSCs at late passages (data not shown). In addition, most abundance classes of mRNAs were reduced in SS-hMSCs during senescence, including the initial triggering of complement (27.8%), complement cascade (27.8%), and the innate immune system (27.8%; Fig. 3D).

Comparison of Serum Proteins

In total, 507 human proteins in serum were analyzed using antibody-based protein arrays for the determination of the differences in serum proteins between healthy subjects and stroke patients. The representative results of serum protein

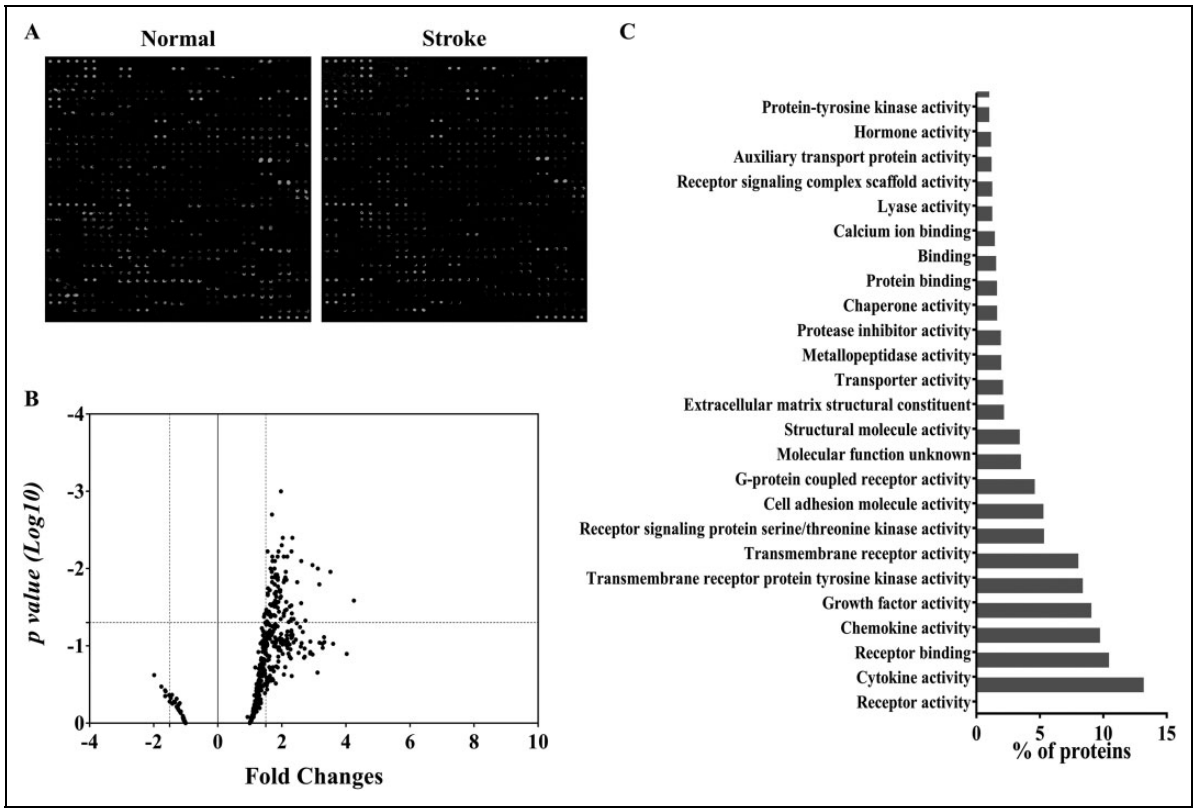

Fig. 4. Comparison of serum protein profiles. (A) Representative images of RayBiotech 507 protein arrays showing the proteome profile of normal healthy control serum and stroke patient serum. (B) Scatter plot representing different protein expression patterns between groups. (C) Molecular functional analysis of selectively increased protein expression in stroke patients' serum using FunRich software.

antibody arrays of healthy subjects and stroke patients are shown in Fig. 4A. Based on the chosen statistical ($P < 0.05$ on t test) and fold change (1.5-fold) cutoff, 88 proteins were identified whose expression was significantly greater in the serum of stroke patients (Fig. 4B; Online Supplementary Table 2). Among them, C-C chemokine receptor type 7 (CCR7; 4.25-fold), lipocalin-2 (LCN-2; 3.5-fold), S100β (3.17-fold), FGF family (FGF basic: 2.31-fold; FGF-BP: 1.64-fold; FGF-5: 2.14-fold; FGF-12: 1.78-fold; and FGF-23: 1.67-fold), VEGF (2-fold), epidermal growth factor (EGF, 1.86-fold), brain-derived neurotrophic factor (BDNF, 1.87-fold), matrix metallopeptidase 9 (MMP-9; 3.17-fold), and fms-like tyrosine kinase 3 ligand (Flt-3L; 2.6-fold) were selected. These proteins were classified according to their molecular function enrichment using the FunRich software. The upregulated proteins were related to cell communication and signal transduction, including receptor activity, growth factor activity, receptor binding, cytokine activity, chemokine activity, and transmembrane receptor protein tyrosine kinase activity (Fig. 4C).

Comparison of Secreted Proteins from MSCs

A comparison of secreted proteins was performed using protein antibody arrays. The representative results of secreted protein antibody arrays from both groups are shown in Fig. 5A, in which 86 proteins were identified whose expression significantly differed between SS-hMSCs and NS-hMSCs (Fig. 5B; Online Supplementary Table 3). These included activin A (3.9-fold), artemin (2.4-fold), interleukins (over 1.6-fold), platelet-derived growth factor (PDGF; over 2-fold), and neurotrophin 4 (NT-4; 2.5-fold). The changed proteins were related to chemokine activity, receptor activity, growth factor activity, cytokine activity, transmembrane receptor protein tyrosine kinase activity, G-protein coupled receptor activity, cell adhesion molecule activity, the extracellular matrix structural constituent, serine/threonine kinase activity, and metallopeptidase activity (Fig. 5C).

Improvements in Neurogenesis and Angiogenesis in an Ischemic Stroke Animal Model

To investigate whether SS-hMSCs enhanced neurogenesis or angiogenesis in vivo compared to FBS-hMSCs, NS-hMSCs, or PBS, we performed immunofluorescence staining analysis for neurogenesis and angiogenesis. The physiological parameters evaluated at different time points were not different among the groups for any measures (Table 2). The result of blood gas analysis showed that rats manifested mild alkalosis at 90 min post-MCAO, but the mean value of all physiological parameters was controlled within normal ranges[15,16]. The quantitative analysis for neurogenesis revealed that the

Table 2. Physiological Parameters.

		Sham				PBS Treatment				MSC Treatment			
		Baseline	After Surgery	After reperfusion	After Treatment	Baseline	After MCAO	After Reperfusion	After Treatment	Baseline	After MCAO	After Reperfusion	After Treatment
Relative CBF (%)	Mean	100	80.99	91.18		100	19.48	71.71		100	19.24	75.86	
	SD	26.61	19.99	17.65		14.34	2.09	16.82		31.33	6.19	26.77	
MABP (mmHg)	Mean	94	98			88	102	91.4		91	97	88.4	
	SD	5.57	8.00			3.08	7.84	7.02		7.17	9.27	8.26	
pH	Mean	7.43		7.42	7.4	7.43		7.46	7.49	7.41		7.48	7.46
	SD	0.02		0.03	0.05	0.03		0.02	0.04	0.03		0.05	0.09
pCO_2 (mmHg)	Mean	43.87		45.10	42.73	45.22		35.02	37.02	44.56		35.56	40.90
	SD	1.90		3.80	4.33	3.96		1.70	4.41	2.80		7.43	9.31
pO_2 (mmHg)	Mean	171.00		160.33	188.33	193.40		174.60	185.00	150.80		166.80	260.60
	SD	12.12		3.21	1.53	90.35		4.39	15.33	13.90		11.99	142.57
Na (mmol/L)	Mean	137.67		138.33	138.00	139.20		139.20	138.80	137.60		137.80	135.80
	SD	1.15		0.58	1.00	5.54		1.79	5.31	1.34		0.84	1.10
K (mmol/L)	Mean	4.43		4.60	4.40	4.54		4.06	3.94	4.66		4.50	3.96
	SD	0.12		0.60	0.30	0.42		0.30	0.27	0.23		0.45	0.34
Ca (mmol/L)	Mean	1.32		1.31	1.35	1.38		1.26	1.30	1.34		1.28	1.34
	SD	0.06		0.02	0.02	0.07		0.01	0.04	0.03		0.05	0.08
Glucose (mg/dL)	Mean	254.00		252.67	252.67	288.40		204.80	185.20	263.20		219.00	195.40
	SD	21.93		13.43	20.50	18.28		9.91	11.54	33.18		23.70	23.07
Hct (%PCV)	Mean	37.33		38.33	35.67	38.20		39.20	39.00	38.00		36.20	37.20
	SD	1.53		3.51	2.52	2.17		2.05	2.12	1.22		1.30	1.10
Hb (g/dL)	Mean	12.70		13.03	12.10	12.98		13.32	13.28	12.92		12.30	12.62
	SD	0.56		1.21	0.85	0.73		0.67	0.72	0.45		0.44	0.38

Abbreviations: CBF, cerebral blood flow; MABP, mean arterial blood pressure; Hct, hematocrit; Hb, hemoglobin; MCAO, middle cerebral artery occlusion; SD, standard deviation.

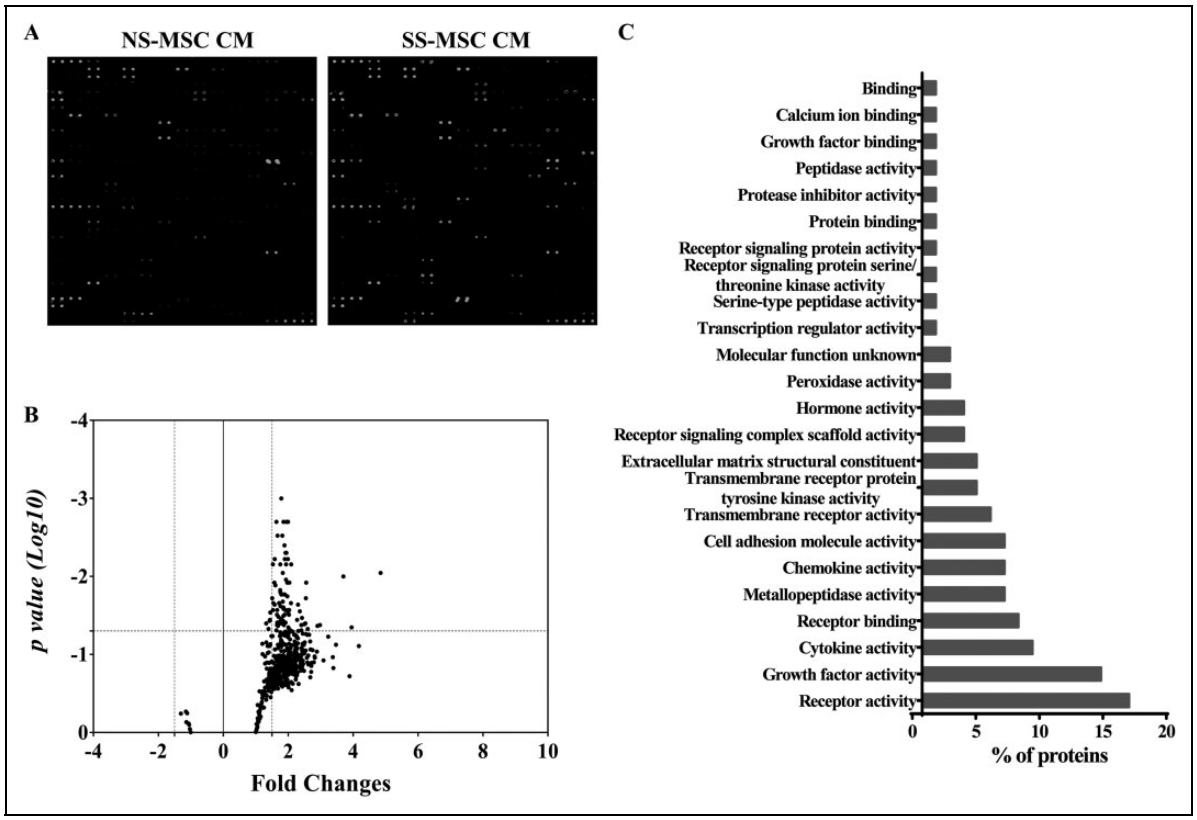

Fig. 5. Comparative analysis of paracrine factor. (A) Representative images of RayBiotech 507 protein arrays showing the proteome profile of conditioned medium of normal healthy control serum human mesenchymal stem cells (hMSCs) and stroke patient serum (SS). (B) Scatter plot representing different protein expression patterns between groups. (C) Molecular functional analysis of selectively increased protein expression in SS-hMSCs conditioned medium using the FunRich software.

number of BrdU/DCX-positive cells was significantly higher in the SS-hMSC group than in the PBS or FBS-hMSC groups at 5 wk after tMCAO (Fig. 6A and B; $*P < 0.05$). The vWF-positive area was significantly greater in the SS-hMSC group than in the PBS, FBS-hMSC, or NS-hMSC groups at 5 wk after tMCAO (Fig. 6C and D; $*P < 0.05$).

Neurological functional recovery was assessed serially using mNSS for up to 35 d (Fig. 6E). All hMSC-treated rats showed significant functional improvements compared to the PBS group at 35 d (PBS: 5.57 $\pm$ 1.13; FBS-MSCs: 4.42 $\pm$ 0.53; NS-MSCs: 4.29 $\pm$ 0.75; and SS-MSCs: 3.14 $\pm$ 0.69). However, functional improvement was most prominent in rats that received SS-hMSCs intravenously (indicated by 2-way ANOVA $F = 4.482$, $P < 0.0001$); early improvement at 21 and 28 d after treatment was observed only in the SS-hMSC group ($**P < 0.01$). The SS-hMSC group showed significant improvement compared to the FBS-hMSC or NS-hMSC groups ($^{\ddagger}P < 0.01$). No significant differences were found between the FBS-hMSC and NS-hMSC groups.

To test whether the infarct volume or atrophy was reduced after hMSC transplantation, MR imaging analysis was performed serially (Fig. 7A). Although the infarct volume was not different among the group at day 1 and 2 wk (Fig. 7B), a significant reduction in relative ventricle volume expansion was observed in the SS-hMSC-treated group (0.98 $\pm$ 0.31) at 2 wk post-tMCAO compared with the PBS-treated group (1.49 $\pm$ 0.40; indicated by 2-way ANOVA, $F = 3.238$, $P < 0.05$ interaction between day and treatment, post hoc analysis by Tukey's analysis, $*P = 0.02$; Fig. 7C).

Discussion

The main findings of this study are that (a) MSCs cultured with stroke patients' serum exhibit higher proliferation indices than MSCs grown in a conventional method (DMEM with 10% FBS); (b) several proteins that are related to the activity of receptors, growth factors, or cytokines were increased in stroke patients' serum; and (c) MSCs cultured with stroke patients' serum showed increased expression of trophic factors and decreased senescence and promoted recovery after stroke.

Wake Up the BM-MSCs

Age-related changes in the characteristics of stem cells have been reported, such as decreased proliferation and differentiation capacities of BM-MSCs[17–19]. Most strokes occur in the elderly. Our results showed that MSCs were activated by SS leading to modulation of proliferation and rejuvenation.

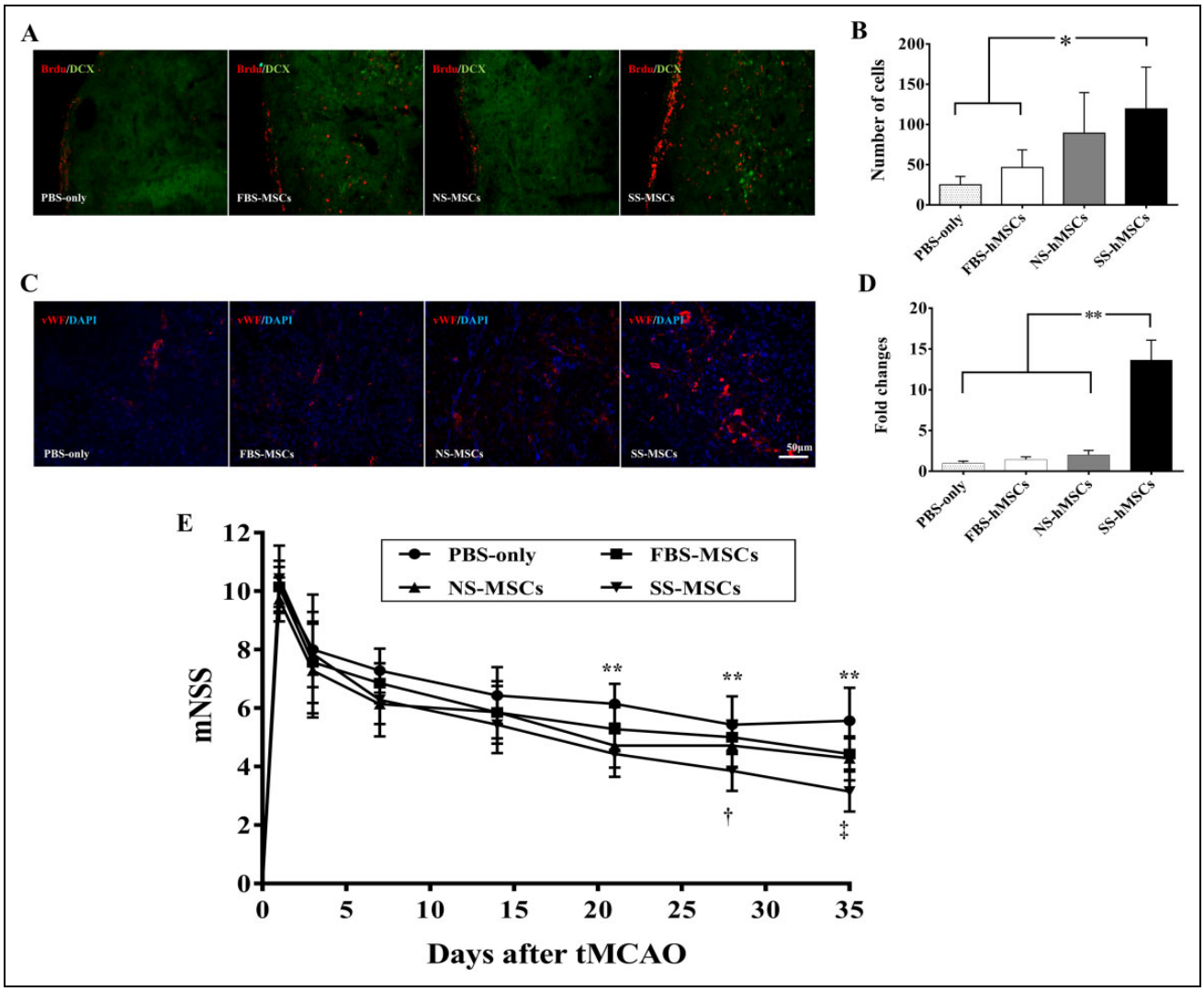

Fig. 6. Neurogenesis and angiogenesis effects of human mesenchymal stem cells (hMSCs) in a stroke rat model. (A) Representative images of immunofluorescence staining with anti-BrdU (red)/anti-doublecortin (DCX; green) for analysis of neurogenesis. (B) Quantitative analysis of neurogenesis expressed as the proliferating cell number with anti-BrdU/anti-DCX positive cells in the subventricular zone. (C) Representative images of immunofluorescence staining with anti-vWF (red)/4',6-diamidino-2-phenylindole (blue) for analysis of angiogenesis. (D) Quantitative analysis of angiogenesis expressed as the anti–von Willebrand factor positive area in the striatum. The quantitation of stained cells was performed in 6 fields per section. The data are presented as mean + SD (*$P < 0.05$). (E) Neurological functional improvements were evaluated in rats that received phosphate buffer solution (PBS), fetal bovine serum (FBS) hMSCs, normal healthy control serum (NS) hMSCs, or stroke patient serum (SS) hMSCs after transient middle cerebral artery occlusion using the modified neurological severity scores scale. Data are expressed as mean + SD (PBS vs. others; **$P < 0.01$, FBS-hMSCs vs. SS-hMSCs; $^{\dagger}P < 0.05$, SS-hMSCs vs. FBS-hMSCs or NS-hMSCs; $^{\ddagger}P < 0.01$, $n = 8$).

This rapid proliferation rate is expressed as an increased percentage of cells in the proliferation phase (S+G2-M phase) and an abbreviated G1 phase (Online Supplementary Fig. 3). In particular, the G1 phase's length is critical in the decision between self-renewal and differentiation and is associated with a loss of stem cell potency[20,21]. Previous studies showed that stroke contributes to the proliferation and mobilization (to the blood) of hematopoietic stem cells (HSCs)[22,23].

Our findings reveal that the expression of cell cycle- and aging-associated mRNAs was in line with the increased proliferation, survival capacity, and reduced cellular senescence of SS-hMSCs. *AURKA* plays a key role in the cell cycle by promoting M-phase entry and progression[24], and activated *AURKA* phosphorylates *BRCA1*, which exhibits tumor-suppressing and DNA-repairing activities[25,26]. *BIRC5* is an inhibitor of apoptosis that can regulate programmed cell death and cell cycles through caspase-9 inactivation and *AURKA* activation[27]. *BUB1b* encodes a kinase involved in mitotic regulation, and its expression is associated with ki-67 expression[28]. A decline in *BUB1b* expression is related to a replicative senescence in adipose-derived MSCs[29], and the overexpression of *BUB1b* can extend healthy life spans and protect against cancer[30]. *TMEM33* codes for a

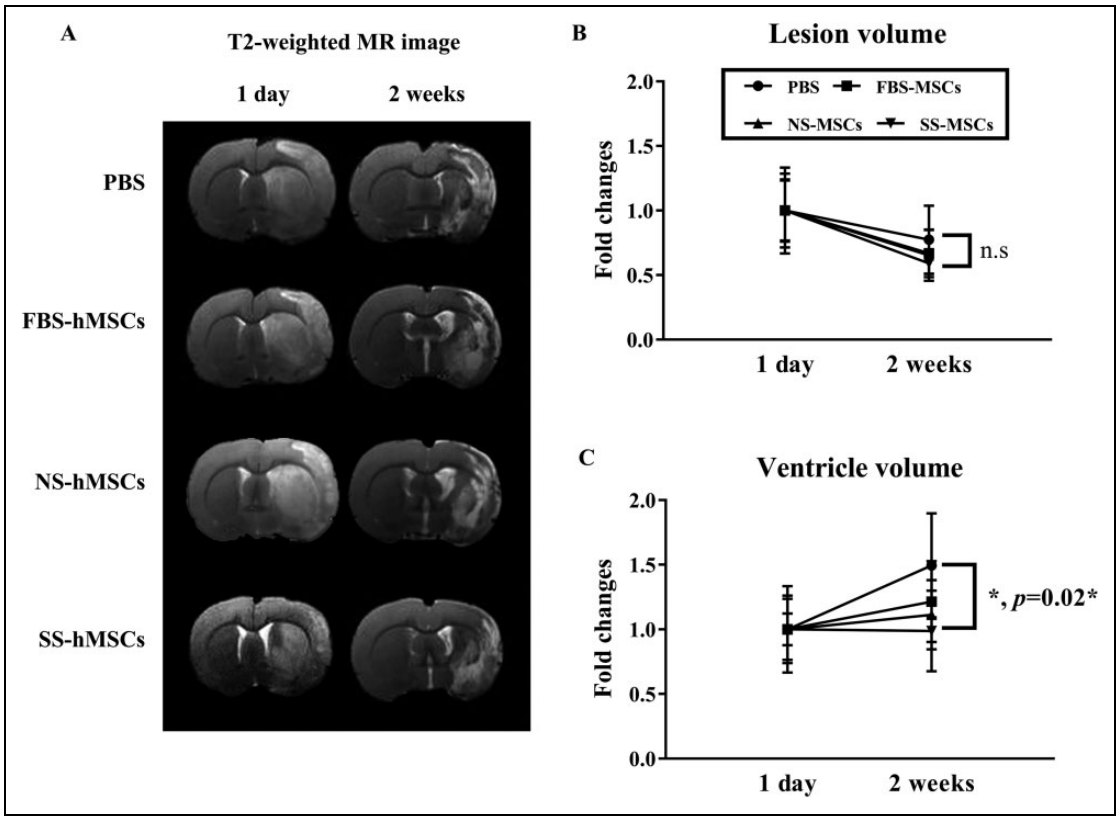

Fig. 7. (A) Representative images of the axial T2-weighted magnetic resonance image scans. Quantitative analysis of the relative lesion volume (B) and ventricle size (C) expressed as the fold changes with bar graph. Data are expressed as mean + SD (*$P = 0.022$).

transmembrane protein located in the endoplasmic reticulum, which can induce the cell death pathway via c-Jun N-terminal kinases (JNK)/p53 pathway activation and *BIRC5* inhibition[31]. *TMEM135*'s function is unknown, but its overexpression can induce the osteoblastogenesis of MSCs[32]. *CDKN1A* codes for p21, a cyclin-dependent kinase inhibitor that can regulate cell cycle progression at G1 via retinoblastoma protein (RB1)[33]. In human cells, an increase in the mRNA level of *CDKN1A* was observed upon stress-induced premature senescence[34]. In our data, the expression of *CDKN1A* in SS-hMSCs was downregulated compared to that of NS-hMSCs by passages 5 to 10. Recently, we have reported that the BM-MSCs of rats with ischemic stroke showed higher levels of miR-20a expression than those of normal rats. Stroke rat serum enhanced the proliferation of rat MSCs via the upregulation of miR-20a, which can regulate the cell cycle by suppressing *CDKN1A*[35]. The expression of immune response genes was reduced in SS-hMSCs in the present study. The increase in immune response genes during senescence, including the associated complementary cascade and the innate immune system, has been found in several different studies[36–38].

Our results showed that serum proteins with various molecular functions, including receptor activity, growth factor activity, cytokine activity, and chemokine activity, were elevated in stroke patients. Some of them are considered putative candidates for improving the therapeutic efficacy of MSCs. The stimulation effects on MSCs with growth factors including VEGF[39], FGF[40], BDNF[41], and EGF[42] have been reported to increase the survival, proliferation, and differentiation of MSCs via the PI3K/Akt pathway[43–45]. LCN-2 is elevated in the blood of ischemic stroke patients[46], and reduces the senescence and cell death of MSCs[47] via the upregulation of various antioxidant and growth factors[48]. MMP-9 is well known as serum biomarker for stroke outcome[49,50], and MMP-9 or MMP activity affects MSC behavior[51–54]. Flt-3L is an essential and nonredundant cytokine for differentiation, migration, and survival of HSCs[55,56] and also for proliferation of MSCs[57,58].

Our results also showed that proteins released from MSCs were different depending on the culture media used. SS-hMSCs released various chemokines, cytokines, and growth factors including activin A, PDGF-B homodimer, and NT-4. Activin A is a multifunctional cytokine associated with enhanced endogenous neurogenesis[59–61]. PDGF-BB is an important paracrine factor of MSCs that modulates endothelial cell proliferation and angiogenesis[62,63]. NT-4 is a member of a neurotrophic factor that promotes neurogenesis[64]. In addition, our recent reports suggested the activation of MSCs with stroke patient's serum leads to increase in mobility of MSCs into ischemic area through modulation of CXCR4 and c-met expression in vitro[65] and proliferation

of MSCs by upregulating microRNA-20a via inhibiting *CDKN1A*[35].

Clinical Application in Stem Cell Therapy for Stroke

Although several stem cell therapies have been applied in stroke patients, there remains some limitations regarding their clinical use. The main limitations of current stem cell therapies include (a) the long culture period required to obtain a sufficient number of stem cells; (b) the death of stem cells within a toxic environment; (c) the limited trophic support for transplanted stem cells; (d) the use of xenogenic serum, with the concomitant risk of transmitting prion diseases and zoonoses[66]; and (e) functional impairment related to stem cell aging, especially when MSCs are obtained via long-term ex vivo culture expansion and in elderly patients[67–69]. In addition, some potential adverse effects of systemic stem cell transplantation were concerned by recent stem cell therapies for stroke patients, such as vascular occlusion by trapping of stem cells in the lung (intravenous applications) or brain vessels (intraarterial applications)[70,71].

MSCs obtained at the time of a stroke's onset may be optimal candidates for use in cell therapy. MSCs derived from stroke patients may be better for this purpose than from healthy donors. The characteristics of BM cells in normal and stroke rats are reportedly different; MSCs from stroke rats promote functional outcomes that may be mediated by enhanced trophic factor and angiogenic characteristics compared to cells from normal rats[5]. Conversely, the characteristics of MSCs from stroke patients could change after the long process of stable culture expansion in FBS, and signals to MSCs in the blood may disappear upon the application of cells[11].

The results of the present study suggest that the culture expansion of MSCs with serum obtained at the acute stage may permit the maintenance of cellular characteristics that are optimal for the neurorestorative treatment of stroke. An MSC culture expansion strategy with serum from stroke patients that optimizes cells to host conditions may be particularly important in cell therapies using relatively "stable" cells such as (a) allogeneic MSCs from nonstroke donors, (b) autologous MSCs used after long-duration storage that have been harvested while in a healthy state, and (c) ex vivo generated cells such as embryonic stem cells or pluripotent stem cells.

Several limitations deserve mention. First, gender difference in stroke incidence, severity, outcome, and response to treatment has been reported[72]. In the present study, we used only male animals to preclude the possible effects of female hormone on MSCs and repair process. Although we followed the recent guidelines for animal research (Online Supplementary Table 2)[73], female animals and animals with stroke risk factors were not used in the present study because female hormones (i.e., estrogen and progesterone) could influence neurogenesis and recovery after stroke[74,75], and circulating female hormones may directly affect the MSC's characteristics[76–78]. Second, in the present, only young healthy animals are used because further studies are needed using aged animals with comorbidity. Third, stroke serum used in this study could not be obtained during the acute phase of stroke because of the ethical issues and possible harmful effect related to blood sampling. However, we additionally performed in vitro studies using samples from stroke rats obtained serially from day 1 to 90th day after tMCAO. We observed that stroke rat serum obtained within 60 d of tMCAO-activated rat MSCs, leading to the modulation of trophic factor expression, proliferation, and survival capacity (Online Supplementary Figs. 2–4). Last but not least, mechanistic study of candidate proteins was not evaluated in the present study. We are currently studying the biologic events responsible for the effects of each protein candidate on the efficacy of MSCs.

Conclusions

Our results indicate that stroke induces a process of recovery via the activation of MSCs. The potential exists for improving the therapeutic efficacy of stem cells, including embryonic stem cells and recently induced pluripotent stem cells. However, strategies to enhance therapeutic efficacy should meet Food and Drug Administration (FDA) regulations regarding stem cells for clinical applications. Given this perspective, the activation of MSCs with autologous serum obtained during the acute phase of a stroke should be considered an effective and feasible method for treating stroke patients.

We have recently initiated the STem cell Application Researches and Trials In NeuroloGy (STARTING)-2 study (clinicalTrials.gov identifier: NCT01716481) in patients with ischemic stroke[6] based on these preclinical results. This clinical trial will determine the effectiveness and safety of autologous MSCs culture expansion in autologous serum obtained from stroke patients as early as possible.

Ethical Approval

This study was approved by the Samsung Medical Center Institutional Review Board, Approval No. SMC 2011-10-047-047.

Statement of Human and Animal Rights

This study was carried out according to the institutional guidelines of the Laboratory Animal Research Center at the Samsung Medical Center.

Statement of Informed Consent

All patients or guardians of patients provided written informed consent to participate in this study.

Declaration of Conflicting Interests

The author(s) declared no potential conflicts of interest with respect to the research, authorship, and/or publication of this article.

Funding

The author(s) disclosed receipt of the following financial support for the research, authorship, and/or publication of this article: This

study was supported by a grant from the Korea Health Technology R&D Project, the Ministry of Health and Welfare (HI14C1624, HI14C3484), and Basic Science Research Program, the Ministry of Science, ICT and Future Planning (NRF-2014R1A1A1004645).

Supplemental Material

Supplementary material for this article is available online.

References

1. Offner H, Subramanian S, Parker SM, Afentoulis ME, Vandenbark AA, Hurn PD. Experimental stroke induces massive, rapid activation of the peripheral immune system. J Cereb Blood Flow Metab. 2006;26(5):654–665.
2. Wolf D, Ley K. Waking up the stem cell niche: how hematopoietic stem cells generate inflammatory monocytes after stroke. Circ Res. 2015;116(3):389–392.
3. Courties G, Herisson F, Sager HB, Heidt T, Ye Y, Wei Y, Sun Y, Severe N, Dutta P, Scharff J, Scadden DT, Weissleder R, Swirski FK, Moskowitz MA, Nahrendorf M. Ischemic stroke activates hematopoietic bone marrow stem cells. Circ Res. 2015;116(3):407–417.
4. Yang B, Xi X, Aronowski J, Savitz SI. Ischemic stroke may activate bone marrow mononuclear cells to enhance recovery after stroke. Stem Cells Dev. 2012;21(18):3332–3340.
5. Zacharek A, Shehadah A, Chen J, Cui X, Roberts C, Lu M, Chopp M. Comparison of bone marrow stromal cells derived from stroke and normal rats for stroke treatment. Stroke. 2010; 41(3):524–530.
6. Kim SJ, Moon GJ, Chang WH, Kim YH, Bang OY, STARTING-2 (STem cell Application Researches and Trials In NeuroloGy-2) collaborators. Intravenous transplantation of mesenchymal stem cells preconditioned with early phase stroke serum: current evidence and study protocol for a randomized trial. Trials. 2013;14(1):317.
7. Lin TM, Tsai JL, Lin SD, Lai CS, Chang CC. Accelerated growth and prolonged lifespan of adipose tissue-derived human mesenchymal stem cells in a medium using reduced calcium and antioxidants. Stem Cells Dev. 2005;14(1):92–102.
8. Hoynowski SM, Fry MM, Gardner BM, Leming MT, Tucker JR, Black L, Sand T, Mitchell KE. Characterization and differentiation of equine umbilical cord-derived matrix cells. Biochem Biophys Res Commun. 2007;362(2):347–353.
9. Pathan M, Keerthikumar S, Ang CS, Gangoda L, Quek CY, Williamson NA, Mouradov D, Sieber OM, Simpson RJ, Salim A, Bacic A, Hill AF, Stroud DA, Ryan MT, Agbinya JI, Mariadason JM, Burgess AW, Mathivanan S. FunRich: an open access standalone functional enrichment and interaction network analysis tool. Proteomics. 2015;15(15):2597–2601.
10. Kim DH, Seo YK, Thambi T, Moon GJ, Son JP, Li G, Park JH, Lee JH, Kim HH, Lee DS, Bang OY. Enhancing neurogenesis and angiogenesis with target delivery of stromal cell derived factor-1 alpha using a dual ionic pH-sensitive copolymer. Biomaterials. 2015;61:115–125.
11. Li WY, Choi YJ, Lee PH, Huh K, Kang YM, Kim HS, Ahn YH, Lee G, Bang OY. Mesenchymal stem cells for ischemic stroke: changes in effects after ex vivo culturing. Cell Transplant. 2008;17(9):1045–1059.
12. Jiang Q, Thiffault C, Kramer BC, Ding GL, Zhang L, Nejad-Davarani SP, Li L, Arbab AS, Lu M, Navia B, Victor SJ, Hong K, Li QJ, Wang SY, Li Y, Chopp M. MRI detects brain reorganization after human umbilical tissue-derived cells (hUTC) treatment of stroke in rat. PLoS One. 2012;7(8):e42845.
13. Paxinos G, Watson C. *The rat brain in stereotaxic coordinates*. Boston (MA): Academic Press/Elsevier; 2007.
14. Bang OY, Lee JS, Lee PH, Lee G. Autologous mesenchymal stem cell transplantation in stroke patients. Ann Neurol. 2005; 57(6):874–882.
15. Hasegawa Y, Morioka M, Hasegawa S, Matsumoto J, Kawano T, Kai Y, Yano S, Fukunaga K, Kuratsu J. Therapeutic time window and dose dependence of neuroprotective effects of sodium orthovanadate following transient middle cerebral artery occlusion in rats. J Pharmacol Exp Ther. 2006;317(2): 875–881.
16. Yavagal DR, Lin B, Raval AP, Garza PS, Dong C, Zhao W, Rangel EB, McNiece I, Rundek T, Sacco RL, Perez-Pinzon M, Hare JM. Efficacy and dose-dependent safety of intra-arterial delivery of mesenchymal stem cells in a rodent stroke model. PLoS One. 2014;9(5):e93735.
17. Bruna F, Contador D, Conget P, Erranz B, Sossa CL, Arango-Rodriguez ML. Regenerative potential of mesenchymal stromal cells: age-related changes. Stem Cells Int. 2016;2016: 1461648.
18. Dufrane D. Impact of age on human adipose stem cells for bone tissue engineering. Cell Transplant. 2017;26(9): 1496–1504.
19. Ganguly P, El-Jawhari JJ, Giannoudis PV, Burska AN, Ponchel F, Jones EA. Age related changes in bone marrow mesenchymal stromal cells: a potential impact on osteoporosis and osteoarthritis development. Cell Transplant. 2017;26(9): 1520–1529.
20. Calegari F, Huttner WB. An inhibition of cyclin-dependent kinases that lengthens, but does not arrest, neuroepithelial cell cycle induces premature neurogenesis. J Cell Sci. 2003;116(Pt 24):4947–4955.
21. Caviness VS Jr., Nowakowski RS, Bhide PG. Neocortical neurogenesis: morphogenetic gradients and beyond. Trends Neurosci 2009;32(8):443–450.
22. Machalinski B, Paczkowska E, Koziarska D, Ratajczak MZ. Mobilization of human hematopoietic stem/progenitor-enriched CD34+ cells into peripheral blood during stress related to ischemic stroke. Folia Histochem Cytobiol. 2006; 44(2):97–101.
23. Gojska-Grymajlo A, Nyka WM, Zielinski M, Jakubowski Z. CD34/CXCR4 stem cell dynamics in acute stroke patients. Folia Neuropathol. 2012;50(2):140–146.
24. Nikonova AS, Astsaturov I, Serebriiskii IG, Dunbrack RL Jr., Golemis EA. Aurora A kinase (AURKA) in normal and pathological cell division. Cell Mol Life Sci. 2013;70(4): 661–687.
25. Sankaran S, Crone DE, Palazzo RE, Parvin JD. Aurora-A kinase regulates breast cancer associated gene 1 inhibition of

centrosome-dependent microtubule nucleation. Cancer Res. 2007;67(23):11186–11194.
26. Zhang J, Powell SN. The role of the BRCA1 tumor suppressor in DNA double-strand break repair. Mol Cancer Res. 2005; 3(10):531–539.
27. Cheung CH, Huang CC, Tsai FY, Lee JY, Cheng SM, Chang YC, Huang YC, Chen SH, Chang JY. Survivin—biology and potential as a therapeutic target in oncology. Onco Targets Ther. 2013;6:1453–1462.
28. Grabsch H, Takeno S, Parsons WJ, Pomjanski N, Boecking A, Gabbert HE, Mueller W. Overexpression of the mitotic checkpoint genes BUB1, BUBR1, and BUB3 in gastric cancer—association with tumour cell proliferation. J Pathol. 2003;200(1):16–22.
29. Lee J, Lee CG, Lee KW, Lee CW. Cross-talk between BubR1 expression and the commitment to differentiate in adipose-derived mesenchymal stem cells. Exp Mol Med. 2009; 41(12):873–879.
30. Baker DJ, Dawlaty MM, Wijshake T, Jeganathan KB, Malureanu L, van Ree JH, Crespo-Diaz R, Reyes S, Seaburg L, Shapiro V, Behfar A, Terzic A, van de Sluis B, van Deursen JM. Increased expression of BubR1 protects against aneuploidy and cancer and extends healthy lifespan. Nat Cell Biol. 2013;15(1):96–102.
31. Hu R, Zhang X, Hilakivi-Clarke L, Kasid U, Clarke R. Abstract P6-05-01: endoplasmic reticulum resident protein transmembrane protein 33 (TMEM33) induces apoptosis via UPR signaling and autophagy in breast cancer cells. Cancer Research. 2015;75(9 Supplement):P6–05-01.
32. Scheideler M, Elabd C, Zaragosi LE, Chiellini C, Hackl H, Sanchez-Cabo F, Yadav S, Duszka K, Friedl G, Papak C, Prokesch A, Windhager R, Ailhaud G, Dani C, Amri EZ, Trajanoski Z. Comparative transcriptomics of human multipotent stem cells during adipogenesis and osteoblastogenesis. BMC Genomics. 2008;9:340.
33. Harper JW, Adami GR, Wei N, Keyomarsi K, Elledge SJ. The p21 Cdk-interacting protein Cip1 is a potent inhibitor of G1 cyclin-dependent kinases. Cell. 1993;75(4):805–816.
34. de Magalhaes JP, Chainiaux F, de Longueville F, Mainfroid V, Migeot V, Marcq L, Remacle J, Salmon M, Toussaint O. Gene expression and regulation in H2O2-induced premature senescence of human foreskin fibroblasts expressing or not telomerase. Exp Gerontol. 2004;39(9):1379–1389.
35. Kim EH, Kim DH, Kim HR, Kim SY, Kim HH, Bang OY. Stroke serum priming modulates characteristics of mesenchymal stromal cells by controlling the expression miRNA-20a. Cell Transplant. 2016;25(8):1489–1499.
36. Naito AT, Sumida T, Nomura S, Liu ML, Higo T, Nakagawa A, Okada K, Sakai T, Hashimoto A, Hara Y, Shimizu I, Zhu W, Toko H, Katada A, Akazawa H, Oka T, Lee JK, Minamino T, Nagai T, Walsh K, Kikuchi A, Matsumoto M, et al.. Complement C1q activates canonical Wnt signaling and promotes aging-related phenotypes. Cell. 2012;149(6): 1298–1313.
37. Anderson DH, Radeke MJ, Gallo NB, Chapin EA, Johnson PT, Curletti CR, Hancox LS, Hu J, Ebright JN, Malek G, Hauser MA, Rickman CB, Bok D, Hageman GS, Johnson LV. The pivotal role of the complement system in aging and age-related macular degeneration: hypothesis re-visited. Prog Retin Eye Res. 2010;29(2):95–112.
38. Reichwald J, Danner S, Wiederhold KH, Staufenbiel M. Expression of complement system components during aging and amyloid deposition in APP transgenic mice. J Neuroinflammation 2009;6:35.
39. Pons J, Huang Y, Arakawa-Hoyt J, Washko D, Takagawa J, Ye J, Grossman W, Su H. VEGF improves survival of mesenchymal stem cells in infarcted hearts. Biochem Biophys Res Commun. 2008;376(2):419–422.
40. Coutu DL, Galipeau J. Roles of FGF signaling in stem cell self-renewal, senescence and aging. Aging (Albany NY). 2011; 3(10):920–933.
41. Singh M, Kakkar A, Sharma R, Kharbanda OP, Monga N, Kumar M, Chowdhary S, Airan B, Mohanty S. Synergistic effect of BDNF and FGF2 in efficient generation of functional dopaminergic neurons from human mesenchymal stem cells. Sci Rep. 2017;7(1):10378.
42. Gharibi B, Hughes FJ. Effects of medium supplements on proliferation, differentiation potential, and in vitro expansion of mesenchymal stem cells. Stem Cells Transl Med. 2012;1(11): 771–782.
43. Chen J, Crawford R, Chen C, Xiao Y. The key regulatory roles of the PI3K/Akt signaling pathway in the functionalities of mesenchymal stem cells and applications in tissue regeneration. Tissue Eng Part B Rev. 2013;19(6):516–528.
44. Tzeng HH, Hsu CH, Chung TH, Lee WC, Lin CH, Wang WC, Hsiao CY, Leu YW, Wang TH. Cell signaling and differential protein expression in neuronal differentiation of bone marrow mesenchymal stem cells with Hypermethylated Salvador/Warts/Hippo (SWH) Pathway Genes. PLoS One. 2015; 10(12):e0145542.
45. Lim JY, Park SI, Oh JH, Kim SM, Jeong CH, Jun JA, Lee KS, Oh W, Lee JK, Jeun SS. Brain-derived neurotrophic factor stimulates the neural differentiation of human umbilical cord blood-derived mesenchymal stem cells and survival of differentiated cells through MAPK/ERK and PI3K/Akt-dependent signaling pathways. J Neurosci Res. 2008; 86(10):2168–2178.
46. Elneihoum AM, Falke P, Axelsson L, Lundberg E, Lindgarde F, Ohlsson K. Leukocyte activation detected by increased plasma levels of inflammatory mediators in patients with ischemic cerebrovascular diseases. Stroke. 1996;27(10): 1734–1738.
47. Bahmani B, Roudkenar MH, Halabian R, Jahanian-Najafabadi A, Amiri F, Jalili MA. Lipocalin 2 decreases senescence of bone marrow-derived mesenchymal stem cells under sublethal doses of oxidative stress. Cell Stress Chaperones. 2014;19(5):685–693.
48. Halabian R, Tehrani HA, Jahanian-Najafabadi A, Habibi Roudkenar M. Lipocalin-2-mediated upregulation of various antioxidants and growth factors protects bone marrow-derived mesenchymal stem cells against unfavorable microenvironments. Cell Stress Chaperones. 2013;18(6):785–800.

49. Kim SJ, Moon GJ, Bang OY. Biomarkers for stroke. J Stroke. 2013;15(1):27–37.
50. Zhong C, Yang J, Xu T, Xu T, Peng Y, Wang A, Wang J, Peng H, Li Q, Ju Z, Geng D, Zhang Y, He J; CATIS Investigators. Serum matrix metalloproteinase-9 levels and prognosis of acute ischemic stroke. Neurology. 2017;89(8):805–812.
51. Kasper G, Glaeser JD, Geissler S, Ode A, Tuischer J, Matziolis G, Perka C, Duda GN. Matrix metalloprotease activity is an essential link between mechanical stimulus and mesenchymal stem cell behavior. Stem Cells. 2007;25(8):1985–1994.
52. Almalki SG, Agrawal DK. Effects of matrix metalloproteinases on the fate of mesenchymal stem cells. Stem Cell Res Ther. 2016;7(1):129.
53. Hawinkels LJ, Zuidwijk K, Verspaget HW, de Jonge-Muller ES, van Duijn W, Ferreira V, Fontijn RD, David G, Hommes DW, Lamers CB, Sier CF. VEGF release by MMP-9 mediated heparan sulphate cleavage induces colorectal cancer angiogenesis. Eur J Cancer. 2008;44(13):1904–1913.
54. Heissig B, Hattori K, Dias S, Friedrich M, Ferris B, Hackett NR, Crystal RG, Besmer P, Lyden D, Moore MA, Werb Z, Rafii S. Recruitment of stem and progenitor cells from the bone marrow niche requires MMP-9 mediated release of kit-ligand. Cell. 2002;109(5):625–637.
55. Stirewalt DL, Radich JP. The role of FLT3 in haematopoietic malignancies. Nat Rev Cancer. 2003;3(9):650–665.
56. Tsapogas P, Mooney CJ, Brown G, Rolink A. The cytokine Flt3-Ligand in normal and malignant hematopoiesis. Int J Mol Sci. 2017;18(6). pii: E1115. doi: 10.3390/ijms18061115.
57. Guo CM, Chan KYW, Cheang P, Hui KM, Ho IAW, Lam PYP. Flt3 ligand expanded bone marrow mesenchymal stem cells for cartilage tissue engineering. Cell Research. 2008;18:S56–S56.
58. Oubari F, Amirizade N, Mohammadpour H, Nakhlestani M, Zarif MN. The important role of FLT3-L in ex vivo expansion of hematopoietic stem cells following co-culture with mesenchymal stem cells. Cell J. 2015;17(2):201–210.
59. Kan I, Barhum Y, Melamed E, Offen D. Mesenchymal stem cells stimulate endogenous neurogenesis in the subventricular zone of adult mice. Stem Cell Rev. 2011;7(2):404–412.
60. Maltman DJ, Hardy SA, Przyborski SA. Role of mesenchymal stem cells in neurogenesis and nervous system repair. Neurochem Int. 2011;59(3):347–356.
61. Abdipranoto-Cowley A, Park JS, Croucher D, Daniel J, Henshall S, Galbraith S, Mervin K, Vissel B. Activin A is essential for neurogenesis following neurodegeneration. Stem Cells. 2009;27(6):1330–1346.
62. Robinson ST, Douglas AM, Chadid T, Kuo K, Rajabalan A, Li H, Copland IB, Barker TH, Galipeau J, Brewster LP. A novel platelet lysate hydrogel for endothelial cell and mesenchymal stem cell-directed neovascularization. Acta Biomater. 2016;36:86–98.
63. Gehmert S, Gehmert S, Hidayat M, Sultan M, Berner A, Klein S, Zellner J, Muller M, Prantl L. Angiogenesis: the role of PDGF-BB on adipose-tissue derived stem cells (ASCs). Clin Hemorheol Microcirc. 2011;48(1):5–13.
64. Shen Y, Inoue N, Heese K. Neurotrophin-4 (ntf4) mediates neurogenesis in mouse embryonic neural stem cells through the inhibition of the signal transducer and activator of transcription-3 (stat3) and the modulation of the activity of protein kinase B. Cell Mol Neurobiol. 2010;30(6):909–916.
65. Bang OY, Moon GJ, Kim DH, Lee JH, Kim S, Son JP, Cho YH, Chang WH, Kim YH, STARTING-2 Trial Investigators. Stroke induces mesenchymal stem cell migration to infarcted brain areas via CXCR4 and C-Met signaling. Transl Stroke Res. 2017 May 25. doi: 10.1007/s12975-017-0538-2. [Epub ahead of print].
66. Spees JL, Gregory CA, Singh H, Tucker HA, Peister A, Lynch PJ, Hsu SC, Smith J, Prockop DJ. Internalized antigens must be removed to prepare hypoimmunogenic mesenchymal stem cells for cell and gene therapy. Mol Ther. 2004;9(5):747–756.
67. Lee JJ, Nam CE, Kook H, Maciejewski JP, Kim YK, Chung IJ, Park KS, Lee IK, Hwang TJ, Kim HJ. Constitution and telomere dynamics of bone marrow stromal cells in patients undergoing allogeneic bone marrow transplantation. Bone Marrow Transplant. 2003;32(9):947–952.
68. Rombouts WJ, Ploemacher RE. Primary murine MSC show highly efficient homing to the bone marrow but lose homing ability following culture. Leukemia. 2003;17(1):160–170.
69. Boltze J, Arnold A, Walczak P, Jolkkonen J, Cui L, Wagner DC. The dark side of the force—constraints and complications of cell therapies for stroke. Front Neurol. 2015;6:155.
70. Pendharkar AV, Chua JY, Andres RH, Wang N, Gaeta X, Wang H, De A, Choi R, Chen S, Rutt BK, Gambhir SS, Guzman R. Biodistribution of neural stem cells after intravascular therapy for hypoxic-ischemia. Stroke. 2010;41(9):2064–2070.
71. Chen J, Li Y, Wang L, Zhang Z, Lu D, Lu M, Chopp M. Therapeutic benefit of intravenous administration of bone marrow stromal cells after cerebral ischemia in rats. Stroke. 2001;32(4):1005–1011.
72. Haast RA, Gustafson DR, Kiliaan AJ. Sex differences in stroke. J Cereb Blood Flow Metab. 2012;32(12):2100–2107.
73. Vahidy F, Schabitz WR, Fisher M, Aronowski J. Reporting standards for preclinical studies of stroke therapy. Stroke. 2016;47(10):2435–2438.
74. Li J, Siegel M, Yuan M, Zeng Z, Finnucan L, Persky R, Hurn PD, McCullough LD. Estrogen enhances neurogenesis and behavioral recovery after stroke. J Cereb Blood Flow Metab. 2011;31(2):413–425.
75. Zheng J, Zhang P, Li X, Lei S, Li W, He X, Zhang J, Wang N, Qi C, Chen X, Lu H, Liu Y. Post-stroke estradiol treatment enhances neurogenesis in the subventricular zone of rats after permanent focal cerebral ischemia. Neuroscience. 2013;231:82–90.
76. Hong L, Zhang G, Sultana H, Yu Y, Wei Z. The effects of 17-beta estradiol on enhancing proliferation of human bone marrow mesenchymal stromal cells in vitro. Stem Cells Dev. 2011;20(5):925–931.
77. Ayaloglu-Butun F, Terzioglu-Kara E, Tokcaer-Keskin Z, Akcali KC. The effect of estrogen on bone marrow-derived rat mesenchymal stem cell maintenance: inhibiting apoptosis through the expression of Bcl-xL and Bcl-2. Stem Cell Rev. 2012;8(2):393–401.
78. Sammour I, Somashekar S, Huang J, Batlahally S, Breton M, Valasaki K, Khan A, Wu S, Young KC. The effect of gender on mesenchymal stem cell (MSC) efficacy in neonatal hyperoxia-induced lung injury. PLoS One. 2016;11(10):e0164269.